

Supporting Information

Strain-Insensitive Naphthalene-diimide-based Conjugated Polymers through Sequential Control

Yan-Cheng Lin,^{a,b,†} Kosuke Terayama,^{c,†} Keita Yoshida,^c Ping-Jui Yu,^a Pin-Hsiang Chueh,^a Chen Chueh,^{a,b} Tomoya Higashihara,^{c,} and Wen-Chang Chen^{a,b,*}*

^a Department of Chemical Engineering, National Taiwan University, Taipei 10617, Taiwan

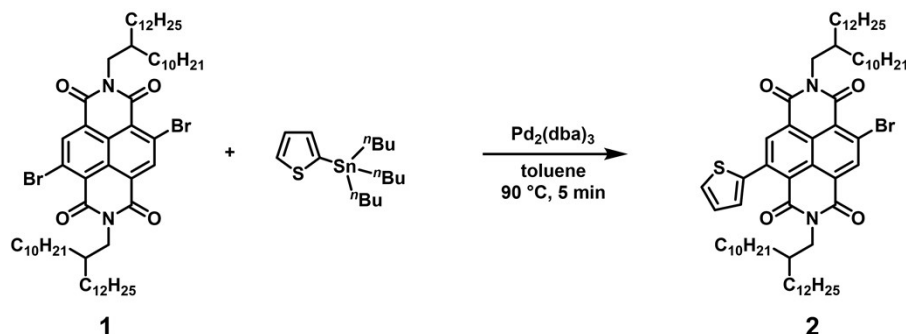
^b Advanced Research Center for Green Materials Science and Technology, National Taiwan University, Taipei 10617, Taiwan

^c Department of Organic Materials Science, Graduate School of Organic Materials Science, Yamagata University, 4-3-16 Jonan, Yonezawa, Yamagata 992-8510, Japan.

*Corresponding authors. E-mail: thigashihara@yz.yamagata-u.ac.jp; chenwc@ntu.edu.tw

[†]They equally contributed to this study as the co-1st authors.

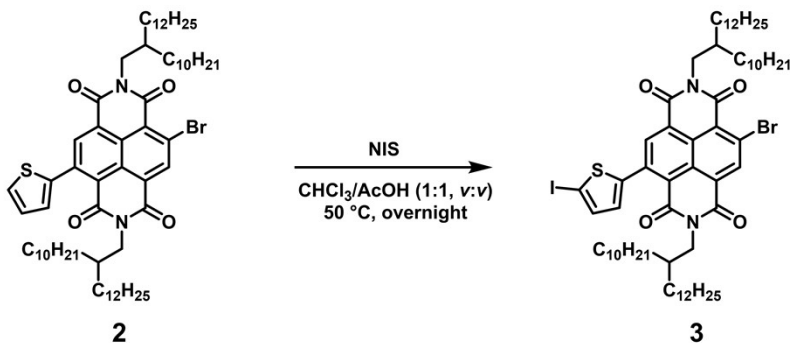
Synthesis of 4-bromo-2,7-bis(2-decyltetradecyl)-9-(thiophen-2-yl)benzo[*lmn*][3,8]phenanthroline-1,3,6,8-tetraone (**2**).



4,9-Dibromo-2,7-bis(2-decyltetradecyl)benzo[*lmn*][3,8]-phenanthroline-1,3,6,8-tetraone (**1**, 8.16 g, 7.44 mmol) and Pd₂(dba)₃ (57.3 mg, 62.6 μmol) were placed in a 100 mL two-necked flask purged with N₂ gas. After dissolving them in deoxidized toluene (40 mL), N₂ was bubbled through the solution for 30 min. 2-(Tributylstannyl)thiophene (2.36 mL, 7.43 mmol) was then added to the mixture, and the solution was stirred at 90 °C for 5 min. The reaction was quenched by adding a 5 M HCl solution (2 mL). The solution was diluted with chloroform and passed through Celite®. The solution was washed with water and KF aqueous solution, dried over anhydrous MgSO₄, filtered, and concentrated under the reduced pressure. The objective compound 4-bromo-2,7-bis(2-decyltetradecyl)-9-(thiophen-2-yl)benzo[*lmn*][3,8]phenanthroline-1,3,6,8-tetraone (**2**) was isolated by silica gel chromatography (hexane : dichloromethane = 2 : 1) in a 12% yield (944 mg) as red solid. ¹H NMR (400 MHz, CDCl₃) δ 8.98 (s, 1H), 8.77 (s, 1H), 7.56 (dd, *J* = 5.1, 1.2 Hz, 1H), 7.29 (dd, *J* = 3.6, 1.2 Hz, 1H), 7.19 (dd, *J* = 5.1, 3.6 Hz, 1H), 4.10 (dd, *J* = 38.6, 7.4 Hz, 4H), 2.07–1.87 (m, 3H), 1.48–1.12 (m, 80H), 0.95–0.81 (m, 12H). ¹³C NMR (100 MHz, CDCl₃) δ 162.15, 162.07, 161.83, 161.42, 140.63, 140.50, 138.89, 137.07, 135.83, 128.42, 128.30, 128.29, 128.26, 127.57, 127.10, 126.24, 124.63, 123.87, 123.70, 45.41, 45.09, 36.56, 36.52, 32.00, 31.64, 31.60, 30.13, 29.78, 29.75, 29.73, 29.72, 29.70, 29.43, 26.44,

26.43, 22.77, 22.75, 14.22. Anal. Calcd. for $C_{66}H_{103}BrN_2O_4S$ (%): C, 72.03, H, 9.43, N, 2.55, S, 2.91. Found (%): C, 72.21, H, 9.49, N, 2.60, S, 2.71.

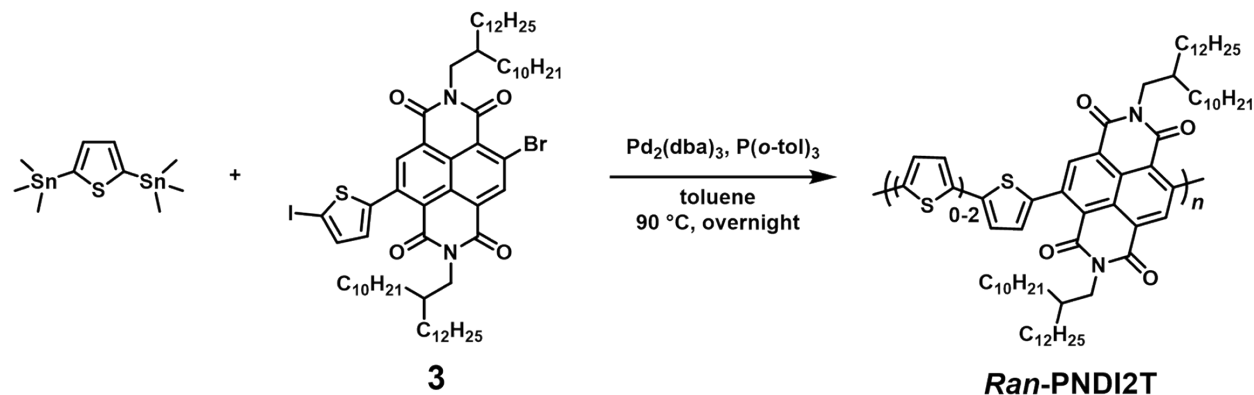
Synthesis of 4-bromo-2,7-bis(2-decyltetradecyl)-9-(5-iodothiophen-2-yl)benzo[lmn][3,8]phenanthroline-1,3,6,8-tetraone (3).



The compound **2** and *N*-iodosuccinimide (96.2 mg, 0.43 mmol) were placed in a 50 mL two-necked flask purged with N_2 gas. After dissolving them in chloroform (10 mL) and acetic acid (10 mL), the mixed solution was stirred at 50 °C overnight. The reaction solution was poured into water (100 mL) and neutralized by adding $NaHCO_3$. The product was extracted with chloroform and the organic layer was washed with water and brine. It was dried over anhydrous $MgSO_4$, filtered, and concentrated under the reduced pressure. The objective compound 4-bromo-2,7-bis(2-decyltetradecyl)-9-(5-iodothiophen-2-yl)benzo[lmn][3,8]phenanthroline-1,3,6,8-tetraone (**3**) was isolated by silica gel chromatography (hexane : dichloromethane = 2 : 1) in a 85% yield (330 mg) as deep red solid. 1H NMR (400 MHz, $CDCl_3$) δ 8.99 (s, 1H), 8.71 (s, 1H), 7.32 (d, $J = 3.8$ Hz, 1H), 6.98 (d, $J = 3.8$ Hz, 1H), 4.10 (dd, $J = 34.1, 7.4$ Hz, 4H), 1.96 (d, $J = 24.2$ Hz, 2H), 1.23 (s, 80H), 0.95–0.81 (m, 12H). ^{13}C NMR (100 MHz, $CDCl_3$) δ 162.19, 162.00, 161.78, 161.38, 146.70, 139.08, 137.34, 136.71, 130.09, 128.59, 128.41, 127.11, 126.25, 124.90, 123.92, 123.53, 45.48, 45.18, 36.60, 32.07, 32.06, 31.69, 31.66, 30.20, 30.18, 29.84,

29.82, 29.79, 29.77, 29.75, 29.51, 29.49, 26.49, 26.46, 22.84, 14.28. Anal. Calcd. for $C_{66}H_{102}BrIN_2O_4S$ (%): C, 64.64, H, 8.38, N, 2.28, S, 2.61. Found (%): C, 64.49, H, 8.19, N, 2.26, S, 2.59.

Stille coupling polycondensation of **3** and 2,5-bis(trimethylstannyl)thiophene.



3 (522 mg, 0.43 mmol), 2,5-bis(trimethylstannyl)thiophene (175 mg, 0.43 mmol), $\text{Pd}_2(\text{dba})_3$ (23.7 mg, 25.9 μmol), and $\text{P}(o\text{-tol})_3$ (66.4 mg, 0.22 mmol) were placed in a 20 mL two-necked flask purged with N_2 gas. After dissolving them in deoxidized toluene (10 mL), N_2 was bubbled through the solution for 30 min. The polymerization was conducted at 90 $^\circ\text{C}$ overnight. 2-(Tributylstannyl)thiophene (0.4 mL, 1.26 mmol) was added and stirred for additional 2 h for the end-capping reaction. The reaction was quenched by adding a 5M HCl solution. The product was extracted with chloroform and the organic layer was washed with water and aqueous KF solution, and passed through Celite[®]. The solution was poured into 300 mL of MeOH to precipitate the polymer. It was filtered and dried under vacuum to afford the objective RA-PNDI2T (466 mg, 93%) as a dark blue solid. SEC: $M_n = 23,400$, $D_M = 3.17$. $^1\text{H NMR}$ (600 MHz, $\text{C}_2\text{D}_2\text{Cl}_4$) δ 9.16 – 8.62 (m, 2H), 7.60 – 7.17 (m, 4H), 4.41 – 3.94 (m, 4H), 2.08 (s, 2H), 1.51 – 1.17 (m, 80H), 0.91 (t, $J = 7.3$ Hz, 12H).

Table S1. Structural, optical, and thermal characterization of the PNDI2T studied.

	M_n^a	M_w/M_n^a	λ_{\max} (nm) ^b	E_g^{opt} (eV) ^c	E_g^{CV} (eV) ^d	HOMO (eV) ^d	LUMO (eV) ^d	T_d (°C) ^e	T_m/T_c (°C) ^f
Alt- PNDI2T	27,000	3.16	395, 710	1.44	2.12	-5.90	-3.78	447	296/ 272
Ran- PNDI2T	23,400	3.17	391, 681	1.44	2.09	-5.88	-3.79	441	200/ 177

^a M_n , M_w , and M_w/M_n were measured by SEC eluted by chloroform. ^b Thin-film UV-Vis absorption maxima. ^c Optical E_g evaluated from the absorption onset of polymer films deposited on quartz substrates. ^d CV determined using Fc/Fc⁺ as an internal potential reference. ^e Determined from TGA at 5% weight loss. ^f Determined from DSC at second heating segment for the melting point (T_m) and first cooling segment for the crystalline temperature (T_c).

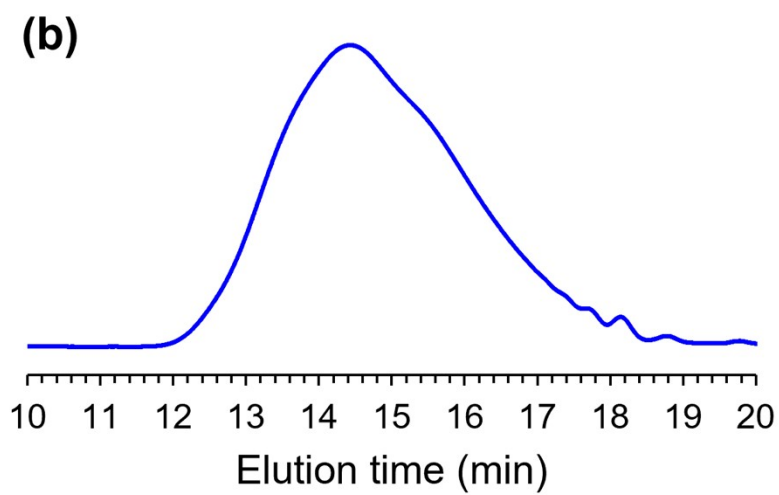
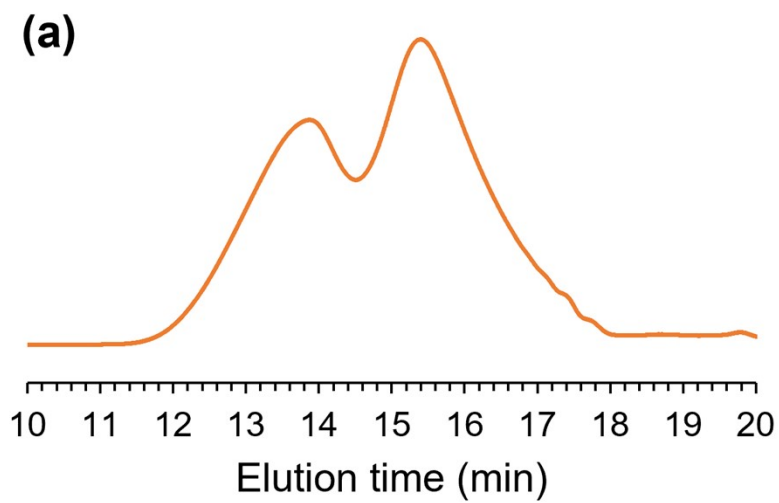


Fig. S1. SEC UV traces of (a) *Alt*-PNDI2T and (b) *Ran*-PNDI2T.

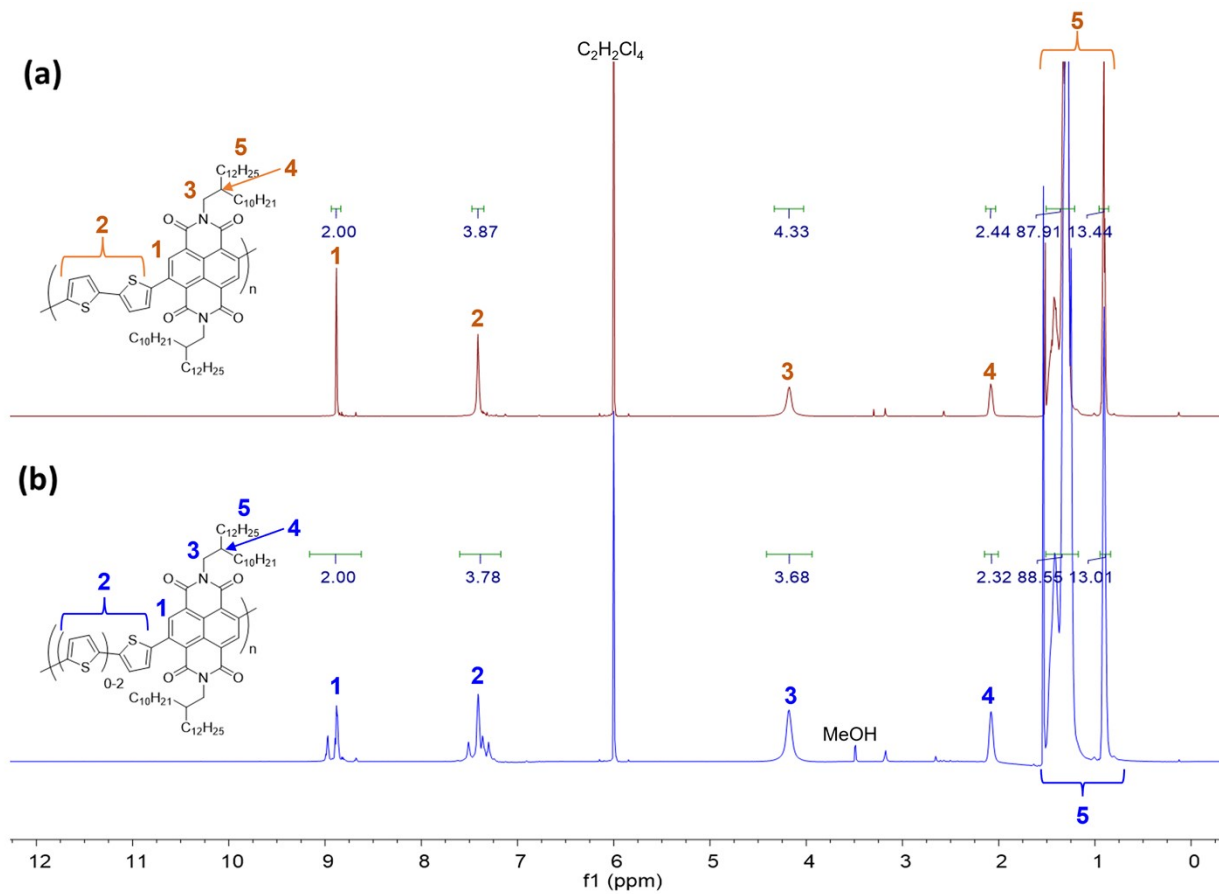


Fig. S2. ^1H NMR spectra of (a) *Alt*-PNDI2T and (b) *Ran*-PNDI2T in $\text{C}_2\text{D}_2\text{Cl}_4$ at 80°C .

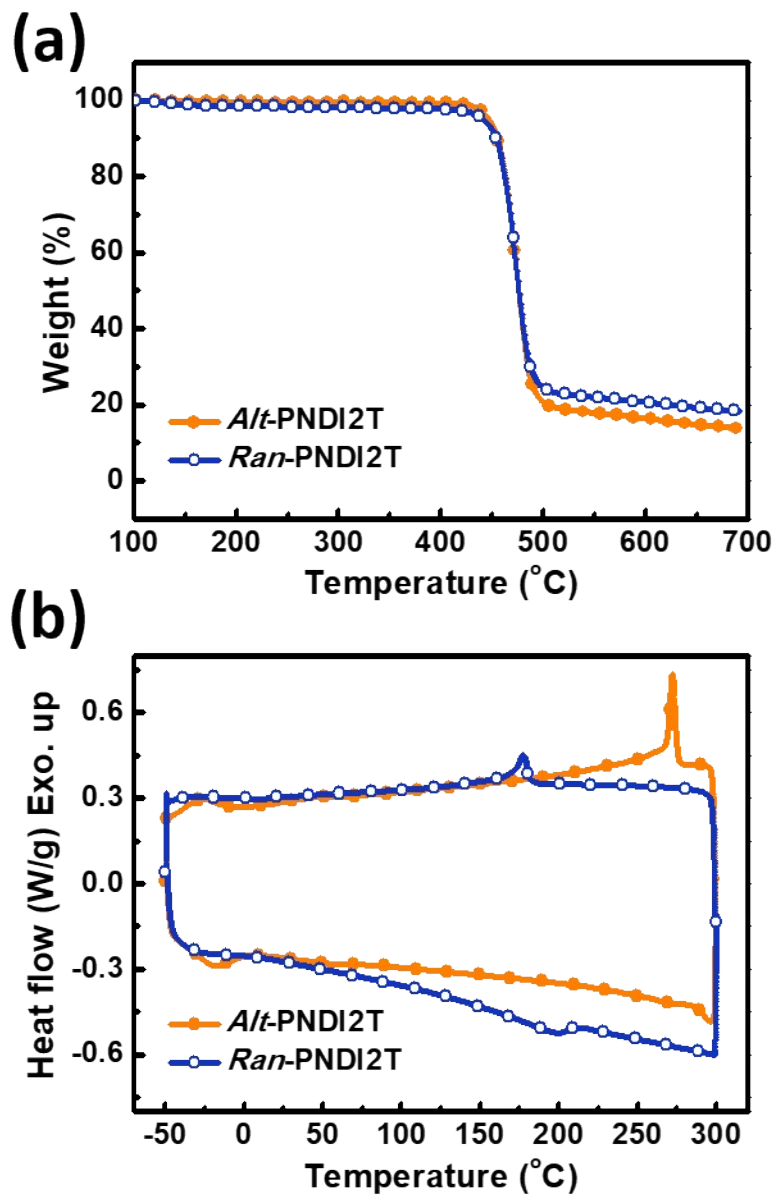


Fig. S3. Thermal analyses of (a) TGA (b) DSC profiles with a ramping rate of 10 °C/min. Note that the DSC profiles are in the first cooling and the second heating segments.

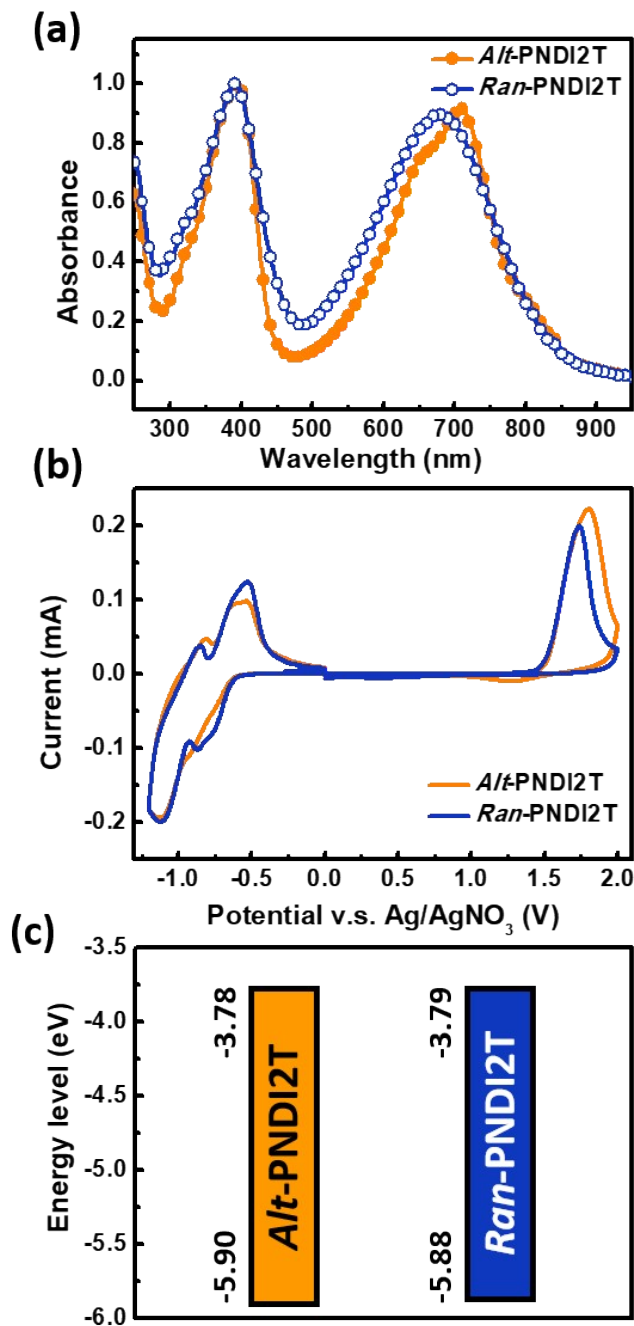


Fig. S4. (a) Film-based UV-vis absorption spectrum, (b) CV profiles and (c) energy level diagram of the PNDI2T studied. Note that the energy levels were evaluated based on the oxidation and reduction onsets in the CV profiles.

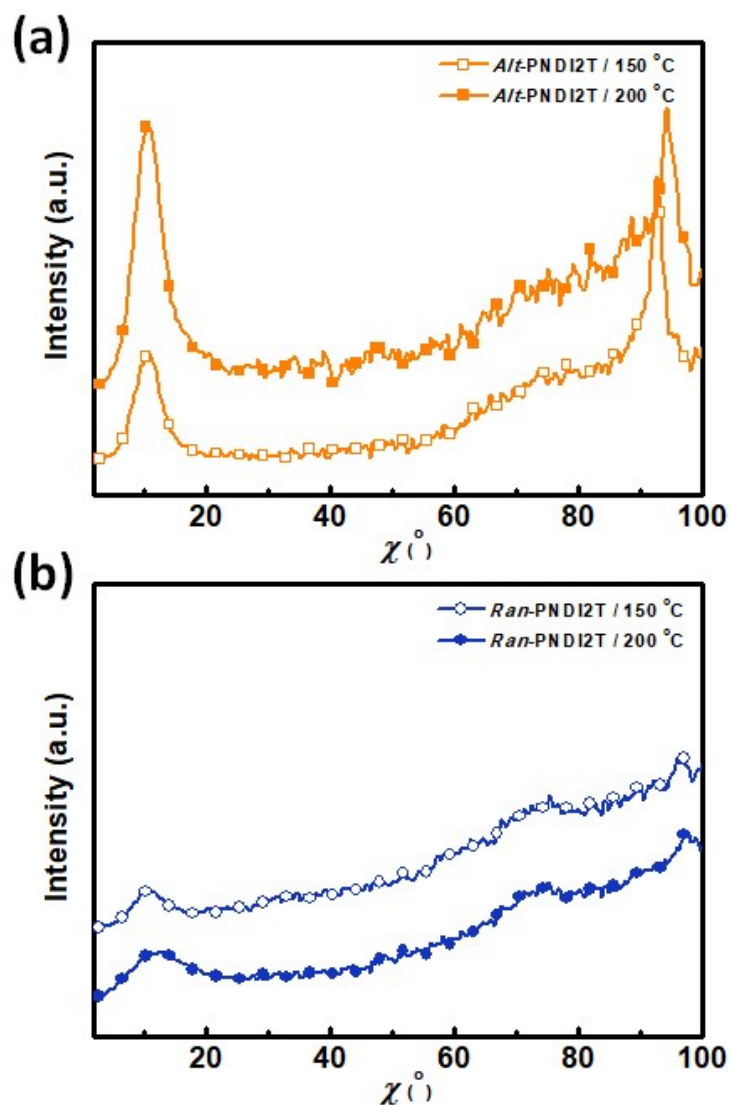


Fig. S5. Pole figures of the out-of-plane (100) peak and in-plane (100) peak of the (a) *A/t*-PNDI2T and (b) *Ran*-PNDI2T films. Note that the geometric corrected intensity was conducted by multiplying $\sin(\chi)$ with the extracted intensity of the (100) diffractions, and the intensity was then divided by exposure time, sample thickness and the beam path length to achieve a normalized intensity.

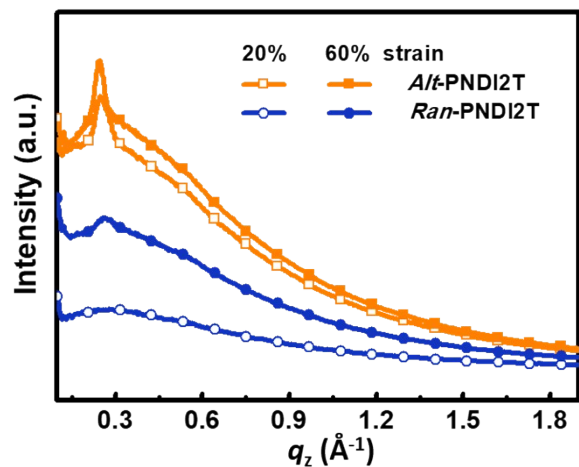


Fig. S6. 1D GIXD profiles in the out-of-plane direction of the transferred/stretched PNDI2T films at varied strain levels.

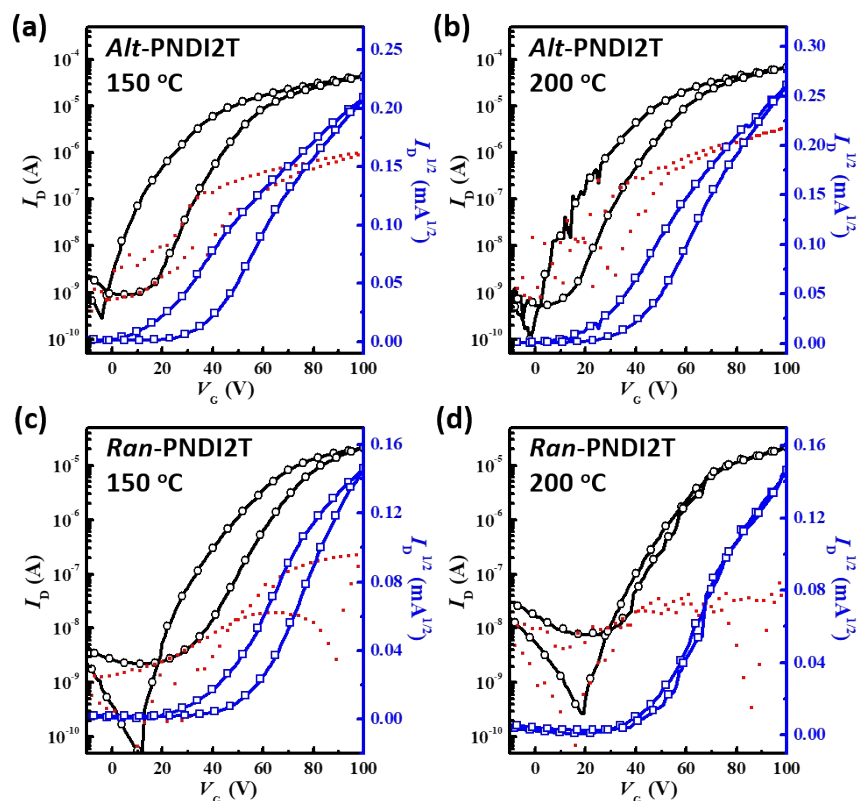


Fig. S7. FET transfer characteristics of the thermally annealed (a,b) *A/t*-PNDI2T (c,d) *Ran*-PNDI2T films at (a,c) 150 °C (b,d) 200 °C.

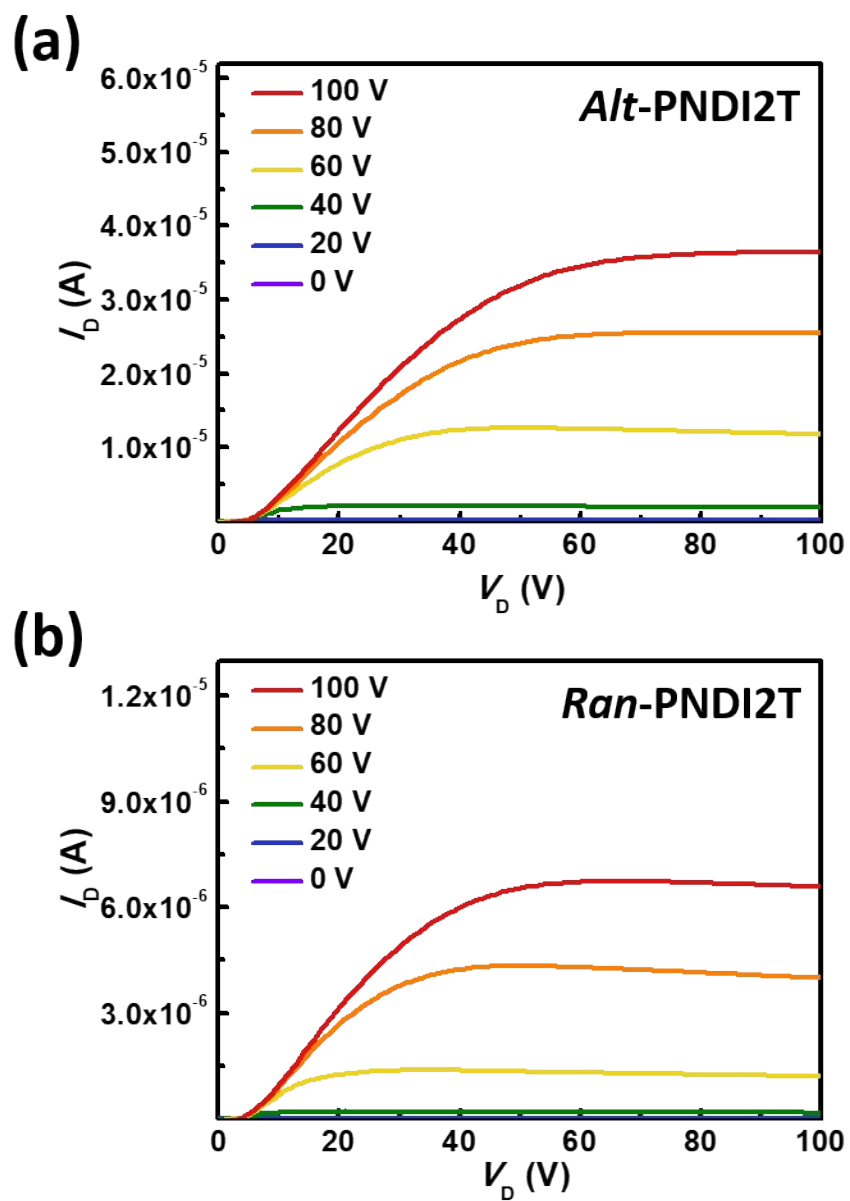


Fig. S8. FET output characteristics of the thermally annealed (a) *Al/t*-PNDI2T (b) *Ran*-PNDI2T films at 150 °C.

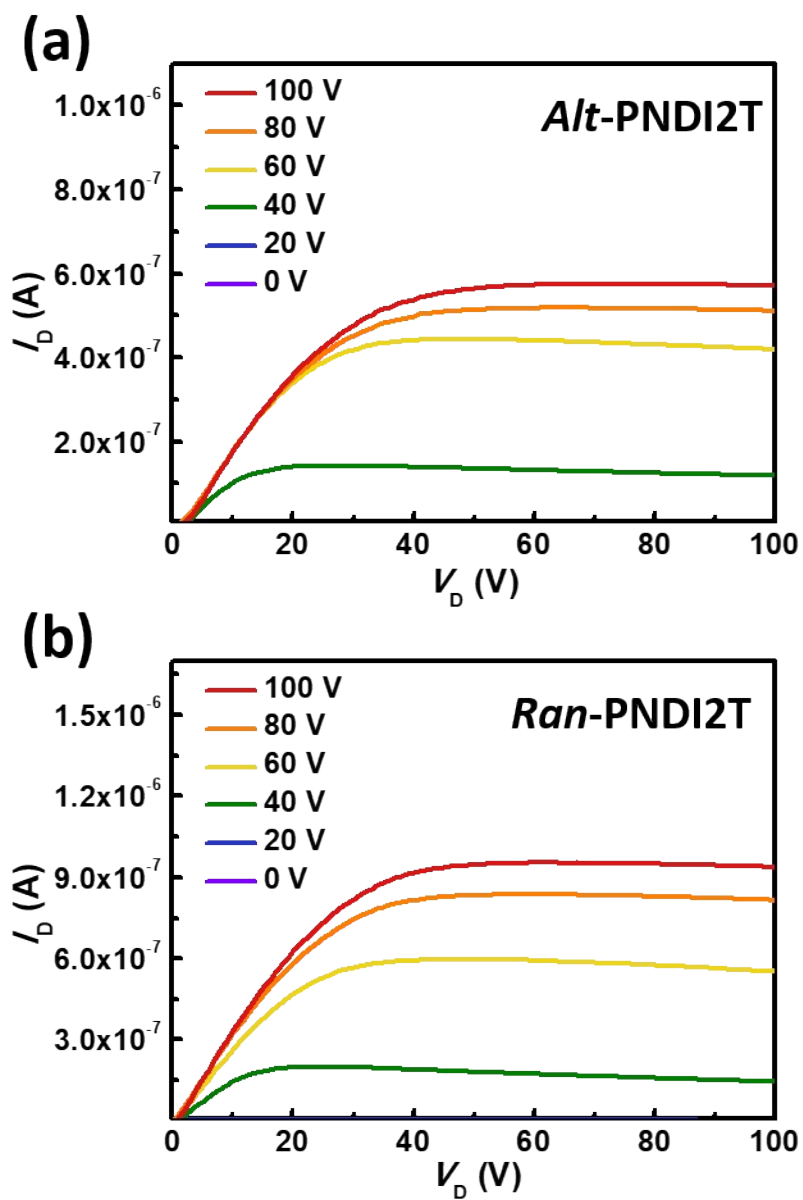


Fig. S9. FET output characteristics of the transferred/stretched (a) *Alt*-PNDI2T (b) *Ran*-PNDI2T films at 60% strain perpendicular to the channel direction.

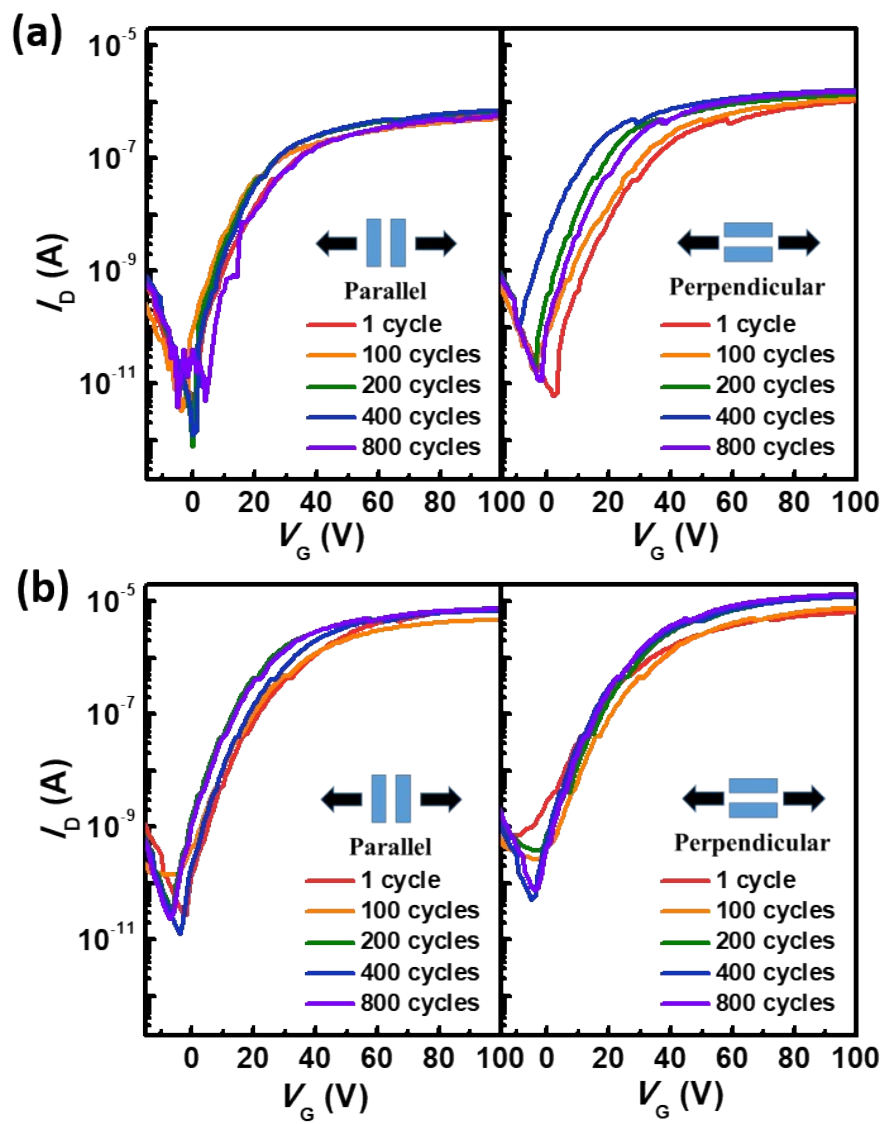


Fig. S10. FET transfer characteristics of the transferred/stretched (a) *Alt*-PNDI2T (b) *Ran*-PNDI2T films after varied stretch-release cycles at 60% strain with the stretch direction parallel (left) or perpendicular (right) to the channel direction.

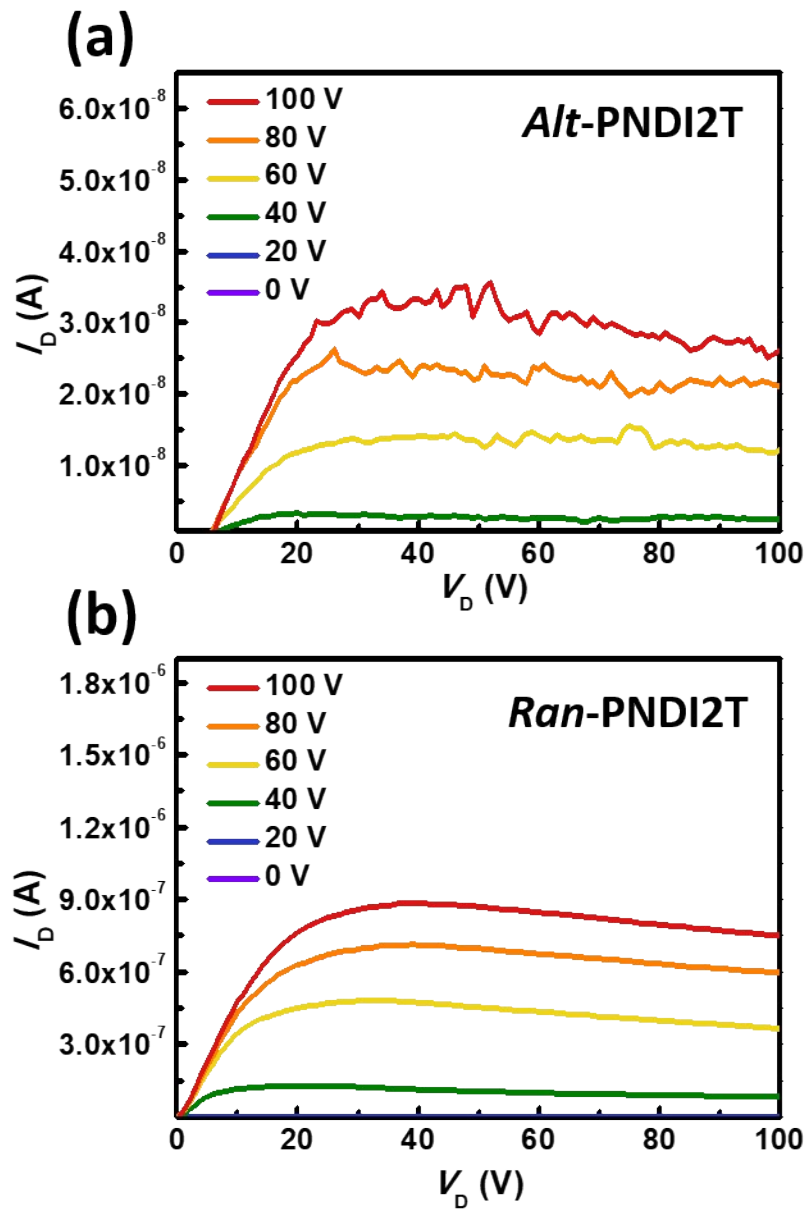


Fig. S11. FET output characteristics of the transferred/stretched (a) *Alt*-PNDI2T (b) *Ran*-PNDI2T films after 800 stretch-release cycles at 60% strain perpendicular to the channel direction.